2017

The Role of Ligand Steric Bulk in New Monovalent Aluminum Compounds

Tomlinson, Warren W.; Mayo, Dennis H.; Wilson, Rebecca M.; Hooper, Joseph P.

ACS Publications

Tomlinson, Warren W., et al. "The Role of Ligand Steric Bulk in New Monovalent Aluminum Compounds." The Journal of Physical Chemistry A 121.24 (2017): 4678-4687. https://hdl.handle.net/10945/71364

THE JOURNAL OF PHYSICAL CHEMISTRY A

Article

pubs.acs.org/JPCA

The Role of Ligand Steric Bulk in New Monovalent Aluminum Compounds

Warren W. Tomlinson,[†] Dennis H. Mayo,[‡] Rebecca M. Wilson,[‡] and Joseph P. Hooper*[,†]

[†]Department of Physics, Naval Postgraduate School, Monterey, California 93943, United States

[‡]Research Department, Naval Surface Warfare Center Indian Head Explosive Ordnance Disposal Technical Division, Indian Head, Maryland 20640, United States

Supporting Information

ABSTRACT: The tetrameric Al(I) cyclopentadienyl compound $Al_4Cp^*_4$ ($Cp^* = C_5Me_5$) is a prototypical low-valence Al compound, with delocalized bonding between four Al(I) atoms and η^5 ligands bound to the cluster exterior. The synthesis of new $[AlR]_4$ ($R = C_5Me_4Pr$, C_5Me_4iPr) tetramers is presented. Though these systems failed to crystallize, comparison of variable-temperature ^{27}Al NMR data with density functional theory (DFT) calculations indicate that these are Al_4R_4 tetramers analogous to $Al_4Cp^*_4$ but with increased ligand steric bulk. NMR, DFT, and Atoms in Molecules analyses show that these clusters are enthalpically more stable as tetramers than the Cp* variant, due in part to noncovalent interactions across the bulkier ligand groups. Thermochemistry calculations for the low-valence metal interactions were found to be extremely sensitive to the DFT methodology used; the M06-2X functional with a cc-pVTZ basis set is shown to provide very accurate values for the enthalpy of tetramerization and ^{27}Al NMR shifts. This computational method is then used to predict geometrical structures, noncovalent ligand interactions, and monomer/tetramer equilibrium in solution for a series of Al(I) cyclopentadienyl compounds of varying steric bulk.

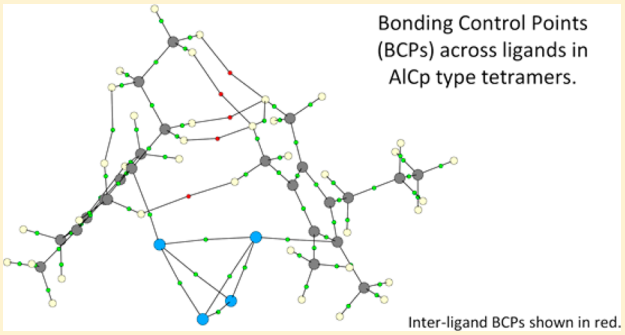

1. INTRODUCTION

Al(I) compounds have received considerable attention in recent years, following the initial synthesis of the monovalent aluminum cluster $Al_4Cp^*_4$ (**1**; Cp* = pentamethylcyclopentadienyl).[1] Investigations on this and similar low-valence aluminum clusters have continued; **1** has served as an aluminum atom source in the formation of nanoparticles, and AlCp* units have proven to be an efficient ligand in many transition-metal complexes.[2−5] Larger clusters with a significant number of low-valence aluminum atoms have also been investigated.[6−10] These systems are of interest for a variety of applications, including use as reagents and precursors for metal−organic chemical vapor deposition.[11,12] We present work here on smaller Al(I) compounds to understand the nature of ligand interactions in these systems.[13]

Currently there are seven synthesized and structurally characterized tetrameric clusters containing a tetrahedral, monovalent aluminum core.[14−20] Of these seven, only two are homoleptic complexes stabilized by a variant of the cyclopentadienyl ligand: $Al_4Cp^*_4$ (**1**) and $Al_4Cp^{\wedge}_4$ (**2**; $Cp^{\wedge} = C_5Me_4H$). The tetramer of the unsubstituted variant, Al_4Cp_4 (**3**; $Cp = C_5H_5$), has been observed in solution but never isolated.[20] Work on these clusters, as well as other low-valence aluminum clusters, is ongoing; as the synthesis and isolation of these materials is difficult, and the final products are often air-sensitive, density functional theory (DFT) analysis has been very helpful in understanding the behavior of these clusters.[21−27] We present here the synthesis of two new aluminum clusters with substituted cyclopentadienyl ligands to explore effects of ligand bulk on their electronic structure and thermochemistry. While these systems failed to crystallize, and unambiguous structural data could not be obtained experimentally, a combination of variable-temperature ^{27}Al NMR experiments and DFT calculations strongly indicate these are tetrameric $Al_4Cp^{*Pr}_4$ (**4**, $Cp^{*Pr} = C_5Me_4Pr$) and $Al_4Cp^{*iPr}_4$ (**5**, $Cp^{*iPr} = C_5Me_4iPr$).

Our main goal is to understand the thermodynamic properties and electronic structure of these clusters as a result of systematic changes in ligand steric bulk. Currently, experimental thermodynamic monomer/tetramer equilibrium data for small Al(I) cyclopentadienyl compounds has only been available for **1**, via van't Hoff analysis of variable-temperature ^{27}Al NMR.[20] Tetramers of **2** and **3** have been observed in solution, but both disproportionate to trivalent aluminum species and bulk metal before AlR monomers are observed. DFT calculations show that Cp^{*Pr} and Cp^{*iPr} variants **4** and **5** are bound into tetrameric forms more strongly than the Cp* variant, despite the addition of steric bulk on the ligands.

Received: March 3, 2017
Revised: May 31, 2017
Published: June 1, 2017

DOI: 10.1021/acs.jpca.7b02075
J. Phys. Chem. A 2017, 121, 4678−4687

Calculations were performed to examine the electronic structure of these clusters and explore changes in bonding with the ligand variations. Our work indicates that calculated thermochemistry for these clusters is very sensitive to the computational methodology, especially the choice of DFT functional. Previous calculations gave a range of results for tetramerization enthalpies and relative stabilities,[20,28] but recent work shows the M06-2X functional has proven to be very accurate in predicting thermodynamic properties and key structural metrics for the two variants with reported solid-state structures (**1** and **2**).[29] We use this computational approach to calculate the most stable isomers of **4** and **5** in the absence of experimental crystallographic data. Further details on determining the lowest-energy geometric configuration are given below. Calculated enthalpy of tetramerization ΔH_{tet} values for these isomers are within 3 kJ/mol of the experimental values measured for the two new compounds. Additionally, we show that M06-2X is also very accurate in predicting ^{27}Al NMR chemical shifts for a variety of low-valence aluminum clusters. Calculated chemical shifts for **4** and **5** are both within 9 ppm of the signals measured for the two new compounds. This strongly suggests that the two new compounds are indeed **4** and **5**. The M06-2X functional was also used to examine the thermodynamic properties for **1**−**3**; our analysis suggests that **3** has a significantly lower tetramerization enthalpy compared to **1**, **2**, **4**, and **5**, despite previous DFT work showing the opposite trend.[20]

A detailed analysis of the bonding was conducted in the context of the Atoms in Molecules (AIM) theory. This analysis shows the importance of noncovalent interactions between the ligands. Several recent studies on similar compounds have also noted the importance of stabilizing dispersion interactions.[30,31] While increased ligand bulk can result in increased Al−Al separation and a reduction in metal−metal bonding in the core, this is often offset by weak interactions between adjacent ligand groups. The tetramerization enthalpies arise from a balance of lone-pair overlap between monovalent Al atoms[28] and noncovalent ligand interactions; this balance is challenging for DFT functionals to capture accurately. Finally, we calculate the constant for monomer/tetramer equilibrium for all five variants. Our calculations indicate that monomers of **2** and **3** are significantly less likely to be found in solution as compared to monomers of **1**, **4**, and **5**.

2. EXPERIMENTAL METHODOLOGY

New cyclopentadienylaluminum derivatives were prepared via thermally activated reductive elimination of tetramethyl(alkyl)-cyclopentadiene from bis(tetramethyl(R)cyclopentadienyl) aluminum hydride intermediates ($Al(C_5Me_4R)_2H$, R = *n*-propyl or *i*-propyl) in toluene at 80 °C (see Scheme 1).[32] Higher-temperature reactions were attempted, but decomposition products were observed in the ^{1}H NMR spectrum when performed above 80 °C. When held at room temperature, solutions of $Al(C_5Me_4R)_2H$ in toluene or benzene are also in equilibrium as observed by ^{27}Al NMR spectroscopy: a solution of $Al(C_5Me_4{}^nPr)_2H$ had an $Al(C_5Me_4{}^nPr)_2H$/**4** ratio of 65:35 after two weeks.

Scheme 1. Synthesis of 4 and 5 via Salt Metathesis and Reductive Elimination

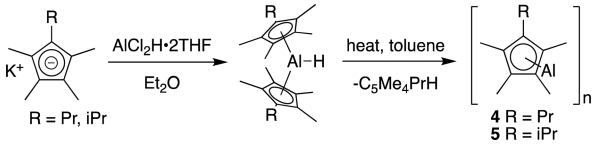

Reductive elimination of cyclopentadienes from Al-$(C_5Me_4R)_2H$ was followed via ^{27}Al NMR spectroscopy. The starting $Al(C_5Me_4R)_2H$ derivatives have diagnostic ^{27}Al NMR signals at ca. −30 ppm; the Cp^{*Pr} and Cp^{*iPr} oligomers, assumed to be tetramer forms, have ^{27}Al signals at −86 and −89 ppm, respectively. For the Cp^{*Pr} variant, multiple cycles of heating followed by removal of the volatile components were necessary. For the Cp^{*iPr} variant, one heat/evaporation cycle was sufficient. The resultant yellow oils and solutions thereof failed to yield crystals suitable for single-crystal X-ray analysis.

The resultant cyclopentadienylaluminum compounds were subjected to variable-temperature van't Hoff analysis. Solutions of the Cp^{*Pr} and Cp^{*iPr} variants in toluene-d_8 were prepared and heated to 80 °C, the ^{27}Al and ^{1}H NMR spectra obtained, and the temperature lowered in 15° increments. Spectra are shown in Figure 1. When heated, the monomer signal grows in intensity (−153 ppm for the Cp^{*Pr} variant, −150 ppm for the Cp^{*iPr} variant), showing a shift in the equilibrium toward monomeric species. The thermodynamic parameters were calculated assuming that the −86 and −89 ppm signals for Cp^{*Pr} and Cp^{*iPr} solutions corresponded to tetrameric forms; attempts to fit the data assuming monomer/dimer equilibrium resulted in considerably worse agreement. Additionally, DFT calculations found no stable dimer or trimer configurations of $AlCp^{*Pr}$ or $AlCp^{*iPr}$. A dimer configuration of AlCp* that was artificially frozen in place was calculated to have an NMR shift of −149 ppm, almost identical to that of the monomeric form. Thus, while we cannot absolutely rule out larger oligomers, all data point to tetrameric Al_4R_4 structures. For the Cp^{*Pr} variant **4**, the enthalpy and entropy changes (ΔH_{tet} and ΔS_{tet}) derived from this analysis are −160 ± 3 kJ/mol and −398 ± 10 J/mol·K, respectively. For the Cp^{*iPr} variant **5**, ΔH_{tet} and ΔS_{tet} are −158 ± 8 kJ/mol and −477 ± 25 J/mol·K. Full experimental details are provided in the Supporting Information.

3. COMPUTATIONAL METHODOLOGY

DFT calculations of all compounds were performed using the Gaussian G09.E01 software.[33] All calculations used an ultrafine grid, and systems were optimized until no imaginary vibrational frequencies were found. Basis set superposition error (BSSE) analysis was done using a counterpoise methodology. Calculations that include explicit dispersion corrections were done using Grimme's D3 approach.[34] Bond critical points and associated density metrics were determined using the DGrid software.[35] To calculate ^{27}Al NMR chemical shifts we plotted known experimental NMR values against the isotropic output from a Gauge-Independent Atomic Orbital (GIAO) calculation scaled by the 0 ppm reference, $Al(H_2O)_6{}^{3+}$.[36] This was done for 17 different low-valent aluminum structures. Eight came from the clusters involved in this study for which we have available NMR data, which includes the monomers and tetramers of **1**, **4**, and **5** and the tetramers of **2** and **3**. The other nine structures were reported by Sitzmann et al.[17]

4. RESULTS AND DISCUSSION

Thermochemistry. It has been challenging to find a reliable computational method for Al(I) cyclopentadienyl compound thermochemistry using ab initio methods, due in large part to a

DOI: 10.1021/acs.jpca.7b02075
J. Phys. Chem. A 2017, 121, 4678−4687

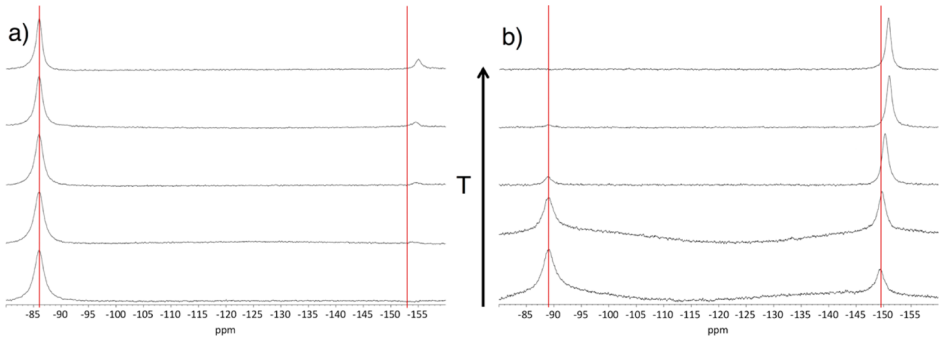

Figure 1. Variable-temperature ^{27}Al NMR of (a) **4** in toluene-d_8 (100 mg in 0.8 mL; 302−347 K) and (b) **5** in toluene-d_8 (44.5 mg in 0.5 mL; 303−353 K).

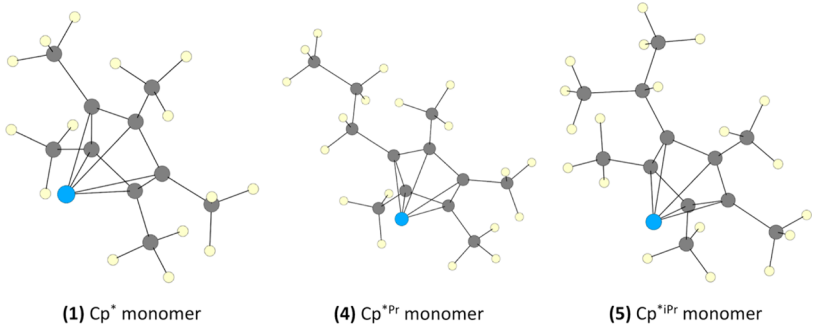

Figure 2. Monomers of three AlR (R = Cp*, Cp*^{Pr}, Cp*^{iPr}) variants. Calculated geometries shown. The aluminum (blue) is positioned in an η^5 configuration in the middle of the carbon (gray) ring.

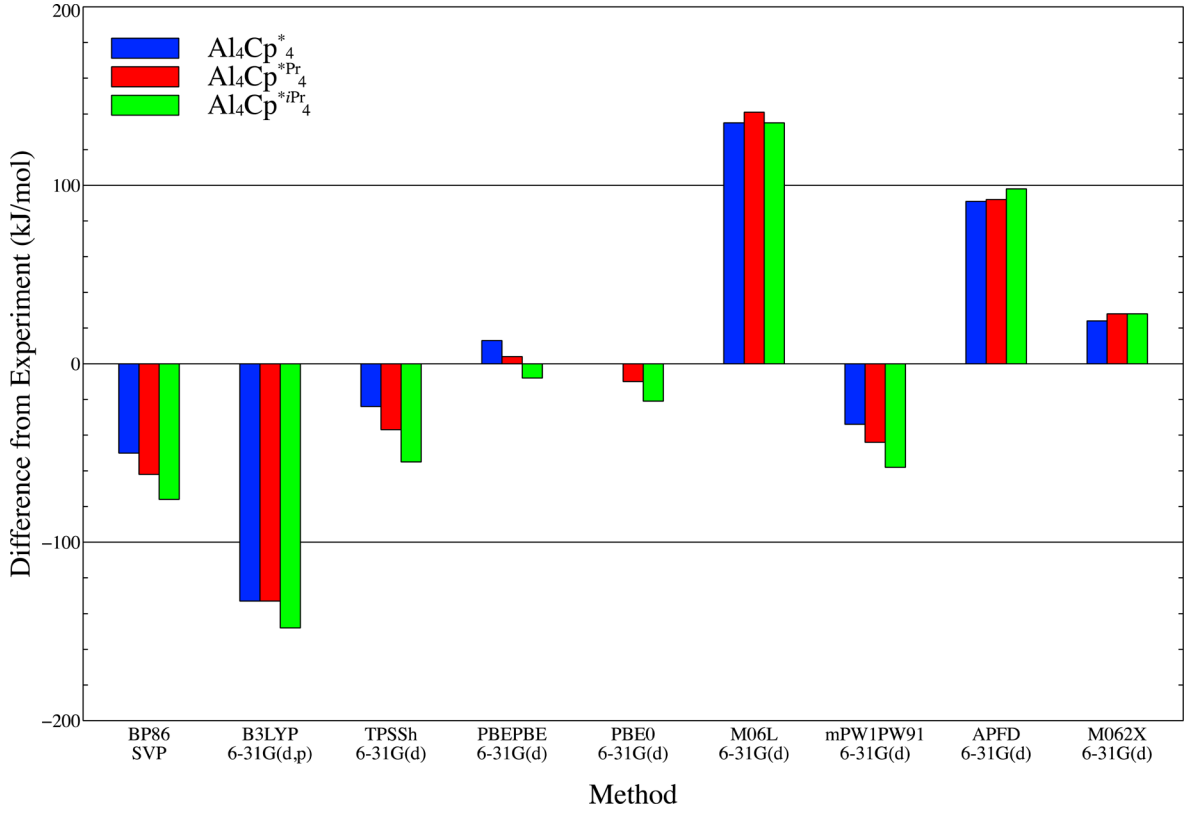

Figure 3. Difference of DFT calculated ΔH_{tet} values from experimental values for various functionals.

lack of experimental data and the difficult synthesis of new clusters of this type. Experimental structural data are only available for the Cp^ and Cp* tetramers and the larger $Al_{50}Cp^*_{12}$, and until now experimental thermochemistry data were only available for the Cp* variant. On the basis of calculated ^{27}Al NMR chemical shifts and ΔH_{tet} values for **4** and

DOI: 10.1021/acs.jpca.7b02075
J. Phys. Chem. A 2017, 121, 4678−4687

5 we work under the assumption that experimental values observed for the two new compounds are indeed tetrameric Cp^{*Pr} and Cp^{*iPr} variants, providing two additional data points for validating the computational accuracy. Previous theoretical treatment of these clusters has produced a range of different results. DFT calculations by Schnöckel and co-workers[20,23] and Williams and Hooper[28] found that **2** and **3** both have stronger tetramerization enthalpies than **1**. This seemed to be supported by the experimental fact that monomers of **2** and **3** were not found via ^{27}Al NMR in solution, but that monomers of **1** were found.[20,21] While geometries and monomer enthalpies of formation were accurately predicted in these works, tetramerization enthalpies were in poor agreement with the experimental results available for **1**. Additionally, new experimental thermochemistry data presented in this paper for both the Cp^{*Pr} and Cp^{*iPr} tetramers suggest these are more stable enthalpically than **1**, even though monomers of each are found in solution. With these new data, we examined the Cp*, Cp^{*Pr}, and Cp^{*iPr} variants with a range of functionals and basis sets[37−48] to demonstrate the large variance of thermochemical results that can result. Monomers of these variants are shown in Figure 2. Multiple configurations of the new Cp^{*Pr} and Cp^{*iPr} variants were examined to determine the global minimum cluster structure. That process is discussed later in the article.

A range of functionals produce accurate results for key geometrical parameters such as the Al−Al distance and the Al−Cp ring-center distance for known systems. Structural parameters for several functionals are given in Table S1 in the Supporting Information, all of which predict key distances to better than 0.05 Å compared to solid-state X-ray data. The thermodynamic results, however, are much more sensitive to the methodology and, in particular, the functional. Figure 3 shows the strong variation of the tetramerization enthalpy with functional type. All three experimental clusters were optimized until no imaginary frequencies were found, and the enthalpy and entropy for the tetramerization reaction was calculated with a double-ζ split valence basis set for computational expediency. Methods used in refs 28 and 20 are also included. Numerical results are presented in Table S3 in the Supporting Information.

Differences in ΔH_{tet} between experiment and theory are as high as 130 kJ/mol, a value sufficient to make equilibrium calculations impossible. Additionally, for all but three functionals, the ordering of ΔH_{tet} for **1**, **4**, and **5** differ from experiment. M06-L and APFD produce the correct relative ordering of tetramers, but both dramatically overpredict ΔH_{tet} for all three structures. The third, M06-2X, has results much closer to experiment. While PBE, PBE0, and M06-2X all perform significantly better than the other methods tested, only M06-2X predicts the correct order of ΔH_{tet} for all three variants. The results for the calculated enthalpy change, ΔS_{tet}, are more mixed. Two methods, BP86 and B3LYP, predict the correct order but have absolute errors of over 100 J/mol·K for the Cp* variant. In general, all tested methods have much higher errors for predicting ΔS_{tet}. This is discussed in more detail below; in what follows we rely on the enthalpy changes to validate predicted structures.

To determine the sensitivity of basis set choice on thermodynamic calculations, we tested the M06-2X functional with eight different basis sets from Pople, Dunning, and Ahlrichs.[49−54] The resulting thermodynamic calculations for ΔH_{tet} and ΔS_{tet}, in addition to experimental results for each of the three variants, are shown in Table S4 of the Supporting Information. While there is not a systematic approach to accurate ΔH_{tet} values with basis set size, the larger cc-PVTZ was chosen as the most accurate available method. To further improve accuracy, basis set superposition error corrections were calculated using a counterpoise technique,[55] and all structures were optimized using a solvent model via the conductor-like screening model (COSMO) as implemented within the Polarizable Continuum Model (PCM) framework for Gaussian.[56,57] Adding an additional D3 dispersion correction resulted in an unphysical overbinding of the clusters; M06-2X has been specifically parametrized to systems containing noncovalent interactions and thus can perform well for systems containing short- to medium-ranged dispersion effects.[39,58−60] Because of the ability of M06-2X/cc-pVTZ to predict ΔH_{tet} to within 3 kJ/mol of experimental values for all variants, we did not perform calculations with basis sets larger than the triple-ζ level. Table 1 shows final calculated ΔH_{tet} values for all five clusters.

Table 1. Calculated[a] ΔH_{tet} Including Basis Set Superposition Error Correction for All Variants

	$Al_4Cp^*_4$	Al_4Cp_4	$Al_4Cp^{\wedge}_4$	$Al_4Cp^{*Pr}_4$	$Al_4Cp^{*iPr}_4$
M06-2X/cc-pVTZ	−148.4	−106.7	−153.1	−158.7	−155.8
experimental	−150			−160	−158

[a]All numbers are in kilojoules per mole.

NMR. In addition to accurate enthalpies of tetramerization, we show that predicted ^{27}Al NMR shifts using the M06-2X functional are quite accurate for known Al(I) compounds. There are eight cyclopentadienyl aluminum structures discussed in this work with experimental ^{27}Al NMR data: the tetramers of **2** and **3** and the monomers and tetramers of **1**, **4**, and **5**. In addition to these eight, experimental NMR data for nine additional related clusters have been reported by Sitzmann and co-workers.[17] We performed GIAO calculations with M06-2X using a 6-31G(d) basis set, and the results show that a static shift of +4.5 ppm brings calculated results into close agreement with experiment. Test calculations with the larger cc-pVTZ basis set using the M06-2X functional showed virtually the same results, but with a slightly larger static shift. The use of other functionals, however, showed strong variations from experiment. Figure S1 in the Supporting Information, for example, shows the poor predictive capability of a functional such as BP86, which was used in previous works. All calculated chemical shifts were normalized by using $Al(H_2O)_6^{3+}$ as the 0 ppm reference. The plot and regression line are shown in Figure 4. As mentioned above, predicted NMR shifts for the $Al_4Cp^{*Pr}_4$ and $Al_4Cp^{*iPr}_4$ are within 9 ppm of the experimentally measured signals for the newly synthesized systems.

Structure of Cp^{*Pr} and Cp^{*iPr} Variants. Solutions of **4** and **5** failed to produce X-ray quality crystals, and thus direct structural information is not available for these two newly synthesized compounds. We therefore performed multiple calculations at the M06-2X/cc-pVTZ DFT level of theory and compared predicted tetramerization enthalpies with variable-temperature NMR experiments. Details of this investigation can be found in the Supporting Information. Calculated ΔH_{tet} values for stable configurations covered a range of ∼23 kJ/mol. The most enthalpically stable configurations of **4** and **5** had calculated ΔH_{tet} values of −158.7 kJ/mol and −155.8 kJ/

DOI: 10.1021/acs.jpca.7b02075
J. Phys. Chem. A 2017, 121, 4678−4687

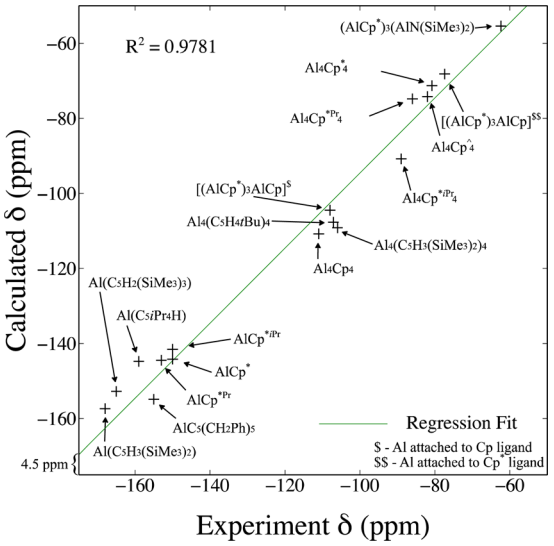

Figure 4. Calculated chemical shifts using M06-2*X*/6-31G(d) compared to experimental data.

mol, respectively. Using this same approach, we also looked at another cluster in this monovalent aluminum series, $Al_4Cp^{*Et}_4$ (**6**; Cp^{*Et} = C_5Me_4Et). While this system has yet to be synthesized, it allows us to analyze trends in the tetramer properties as a function of Cp bulk. The ΔH_{tet} for this cluster is −151.5 kJ/mol, which lies between the Cp* variant and the bulkier tetramers **4** and **5**. Figure 5 shows the most enthalpically stable structures for all six Cp variants, listed in order of increasing steric bulk and annotated with calculated ΔH_{tet} values. Experimental values are also included for **1**, **4**, and **5**.

In general, adding steric bulk within this series results in tetramers with stronger binding, but $Al_4Cp^{\wedge}_4$ is an exception to this trend. Despite the fact that **1** and **6** carry more steric bulk, **2** is more enthalpically stable. Crystal structure data for **2** show that it is configured in the pattern shown in Figure S3b, which differs from the lowest-energy configuration of **4**. DFT calculations for **2** configured to match the lowest-energy configuration of **4** (shown in Figure S3a) differ by only 0.03 kJ/mol. This indicates that the two configurations are essentially degenerate, suggesting that **2** is less sensitive to ligand configuration. Stability gained by interligand interactions can be offset by a loss of Al−Al bond strength due to increased monomer separation within a cluster. To better understand this balance, we consider the electronic structure in more detail.

Atoms in Molecules Analysis. While Al−Al bond length within the core of these clusters can inform overall bond strength, this length does not appear to be good metric for gauging overall cluster stability. The lowest-energy configuration of **5**, for example, has larger Al−Al separation than **1**, **2**, or **3** but is enthalpically preferred. Work done by Stelzer and co-workers demonstrated the existence of attractive noncovalent interactions between adjacent ligands in the Cp* variant.[27] Additionally, Lu and co-workers demonstrated the existence of noncovalent bonding across ligands in the Cp* variant.[29] Here we present atoms in molecules (AIM) analysis to quantify the role of interligand bonding in all variants. AIM analysis involves examining key topological parameters of the electronic density surface of a given molecule. In particular, points where the density gradient vanishes can indicate potential bonds between atoms. The value of electron density and its Laplacian and energy density at these bond critical points (BCPs) can indicate the character of a potential bond. Our analysis shows interligand interactions to be a significant element of overall cluster bonding. Multiple interligand BCPs

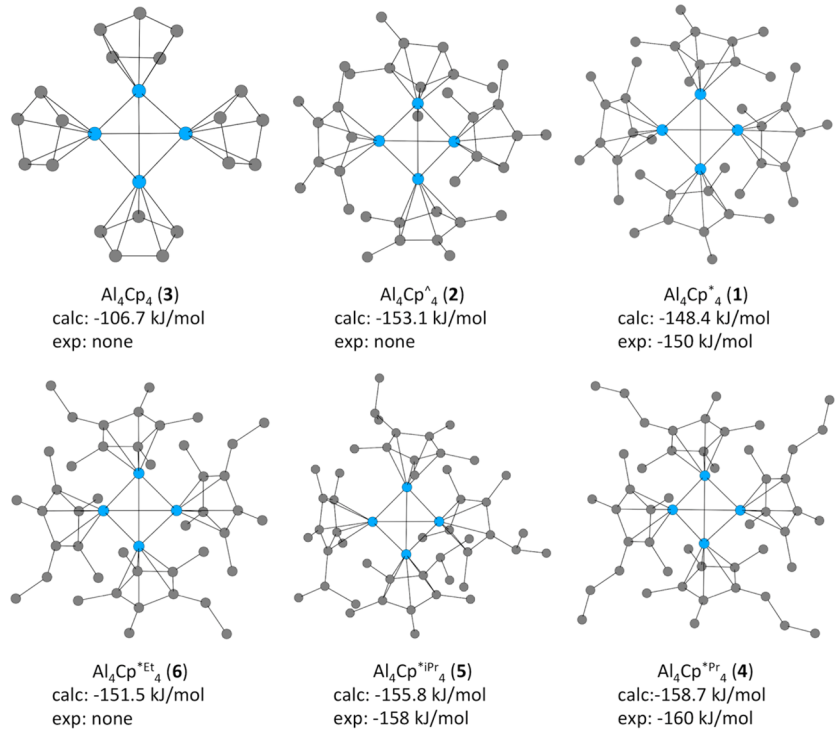

Figure 5. All six variants investigated in order of increasing steric bulk. Calculated and experimental ΔH_{tet} are included. Hydrogens removed for clarity.

DOI: 10.1021/acs.jpca.7b02075
J. Phys. Chem. A 2017, 121, 4678−4687

Table 2. Topological Average BCP Metrics[a] for All Variants

cluster	BCP type	ρ	$\nabla^2\rho$	ε	$\lvert V\rvert/G$	G/ρ	H
Al_4Cp_4	Al−Al	0.0378	−0.0201	0.4400	2.7954	0.1677	−0.0114
	Al−C	0.0348	0.0874	5.1460	1.2596	0.8497	−0.0077
$Al_4Cp^{\wedge}_4$	Al−Al	0.0375	−0.0183	0.5900	2.6580	0.1854	−0.0115
	Al−C	0.0393	0.1193	12.1500	1.2228	0.9708	−0.0085
	H−H	0.0041	0.0131	0.6739	0.7330	0.6240	0.0007
	H−C[b]	0.0043	0.0146	2.1750	0.7050	0.6317	0.0008
$Al_4Cp^*_4$	Al−Al	0.0352	−0.0154	0.5033	2.6057	0.1804	−0.0102
	Al−C	0.0403	0.1205	10.0750	1.2282	0.9678	−0.0089
	H−H	0.0055	0.0184	1.8728	0.7534	0.6564	0.0009
	H−C[b]	0.0062	0.0214	1.3333	0.7523	0.6640	0.0010
$Al_4Cp^{*Et}_4$	Al−Al	0.0353	−0.0153	0.4933	2.5953	0.1822	−0.0103
	Al−C	0.0411	0.1242	4.6325	1.2265	0.9780	−0.0091
	H−H	0.0062	0.0213	1.8215	0.7609	0.6914	0.0010
	H−C[b]	0.0	0.0	0.0	0.0	0.0	0.0
$Al_4Cp^{*iPr}_4$	Al−Al	0.0329	−0.0122	0.4083	2.5212	0.1781	−0.0089
	Al−C	0.038 95	0.108 33	15.798	1.249 25	0.9219	−0.0090
	H−H	0.0063	0.0207	0.8416	0.7729	0.6737	0.0010
	H−C[b]	0.0074	0.0265	1.4044	0.7756	0.7290	0.0012
$Al_4Cp^{*Pr}_4$	Al−Al	0.0352	−0.0153	0.4933	2.5955	0.1815	−0.0102
	Al−C	0.0410	0.1237	4.5800	1.2275	0.9756	−0.0091
	H−H	0.0062	0.0211	1.7895	0.7623	0.6913	0.0010
	H−C[b]	0.0040	0.0140	1.3475	0.7070	0.6868	0.0008

[a]All numbers are in atomic units. [b]Interligand BCPs only.

were found for all except the Cp variant. Key metrics are listed in Table 2, and interligand BCPs for the Cp^{*Pr} variant are shown in Figure 6.

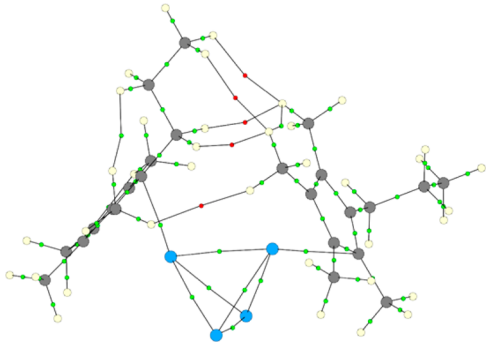

Figure 6. Interligand H−H BCPs in the Cp^{*Pr} variant, shown in red. Remaining BCPs are shown in green.

The information gained through AIM analysis of these clusters gives us insight into the bonding within the tetramers. We see there is a not a simple trend as the steric bulk of the Cp-type ligand increases. It is reasonable to expect that the addition of steric bulk to the ligands of these types of clusters would reduce tetrameric stability, but the opposite is the case. The Cp and $Cp^{\wedge}$ variants have the smallest average Al−Al bond distance at 2.722 and 2.720 Å, respectively, a mere 0.19 pm apart and ∼4.5 pm from the next closest variant. As expected, the total electron density at the six Al−Al BCPs is highest for the Cp and $Cp^{\wedge}$ variants. Table 3 shows a list of average Al−Al bond distance and total electron density at the BCPs associated with these bonds for all six cluster variants as well as two additional configurations: Cp^{*Pr} in the configuration shown in Figure S3b and Cp^{*iPr} in the configuration shown in Figure S3a. These configurations were included because of their varied Al−Al bond distance.

There is a clear correlation between the amount of electron density at the six BCPs joining the core aluminum atoms and the Al−Al average bond distance. A linear fit of a plot of Al−Al bond distance (Figure S6 in the Supporting Information) against total electron density has an R^2 value of over 0.99. These bonds, however, are not the only ones involved in overall cluster stability. The H−H and H−C BCPs found in all substituted Cp derivatives clearly indicate there is additional stability via noncovalent ligand interactions, both in silico and in solution.

The relevant metric for assessing the contributions to stability from the interligand H−H and H−C interligand bonds is the magnitude of electron density at the associated BCPs. Like ρ_b associated with Al−Al bonds, ρ_b associated with these closed-shell bonds can also indicate bond strength.[61,62] It is important to note, however, that similar amounts of electron density at BCP associated with different types of bonds most likely do not indicate that the bonds are of the same strength.[63] The interligand H−H and H−C BCPs in these clusters indicate closed-shell bonds as opposed to the shared Al−Al bonds in the

Table 3. Al−Al Bond Distances and Total Electron Density[a] at BCPs for Eight Cluster Variants

	Cp	$Cp^{\wedge}$	Cp*	Cp^{*Et}	Cp^{*iPr}	Cp^{*Pr}	Cp^{*Pr}[b]	Cp^{*iPr}[c]
Al−Al dist	2.7215	2.7196	2.7684	2.7672	2.8240	2.7670	2.7832	2.8631
ρ_b	0.2269	0.2249	0.2114	0.2116	0.1974	0.2114	0.2074	0.1876

[a]Numbers are in angstroms (or $Å^{-3}$). [b]Orientation show in Figure S3b. [c]Orientation shown in Figure S3a.

DOI: 10.1021/acs.jpca.7b02075
J. Phys. Chem. A 2017, 121, 4678−4687

core. The total amount of electron density associated with each type of bond for each cluster variant is listed in Table 4. These

Table 4. Total Electron Density[a] at Al−Al, H−H, and H−C BCPs for Various Clusters

	total Al−Al ρ_b	total H−H ρ_b	total H−C ρ_b	ΔH_{tet} (calc)
Al_4Cp_4	0.2269	0.0	0.0	−108.6
$Al_4Cp^{\wedge}{}_4$	0.2249	0.0738	0.0086	−161.1
$Al_4Cp^{*}{}_4$	0.2114	0.1066	0.0106	−154.5
$Al_4Cp^{*Et}{}_4$	0.2116	0.1249	0	−157.9
$Al_4Cp^{*iPr}{}_4$	0.1974	0.1193	0.0669	−162.7
$Al_4Cp^{*Pr}{}_4$	0.2114	0.1242	0.0159	−165.7
$(Al_4Cp^{*Pr}{}_4)^b$	0.2074	0.1199	0.0144	−160.0
$(Al_4Cp^{*iPr}{}_4)^c$	0.1876	0.1255	0.0382	−135.6

[a]Numbers are in e·Å^{-3} or kilojoules per mole. [b]Orientation shown in Figure S3b. [c]Orientation shown in Figure S3a.

metrics are listed along with the corresponding BSSE-corrected ΔH_{tet}. No solvent corrections are used, so fundamental trends can be analyzed. Also included are the same two additional configurations examined in the Al−Al bond distance analysis. The value of ΔH_{tet} for these additional configurations provides more overall variance for subsequent regression analysis.

Previous work by Boyd and co-workers demonstrated a linear relationship between ρ_b and bond energy for various types of bonds.[64] We performed a multivariable linear regression of the enthalpy of tetramerization for all clusters in Table 4 based on the summed electron density at Al−Al, H−H, and H−C bond critical points to gain a sense of their relative contributions to tetramer stability. The regression fit, shown visually in Figure S6 in the Supporting Information, is written as

$$\Delta H_{tet} = a_0 + a_1\rho_{Al-Al} + a_2\rho_{H-H} + a_3\rho_{H-C} \quad (1)$$

where ρ_{X-X} is the total electron density at the BCPs associated with X−X bonds for a given cluster. The electron density associated with H−C interligand noncovalent bonds, governed by the coefficient a_3, contributes the least to tetramer stability. The optimal fit gives ratios $a_1/a_3 \approx 3.8$ and $a_2/a_3 \approx 1.3$. Thus, approximately 65% of the variation in tetramer binding energy can be explained by the electron density at Al−Al bond critical points, which varies linearly with Al−Al separation. The remainder can be attributed to interligand effects.

This analysis helps explain why the Cp variant has the weakest binding energy of all clusters considered here, despite having the second-smallest Al−Al bond distance and the largest ρ_b associated with Al−Al bonds. The Cp variant has no interligand H−H or H−C noncovalent bonds and therefore no additional contribution to tetramer stability. Compared to the Cp variant, the Cp^ variant has only a slightly smaller average Al−Al bond distance and slightly less ρ_b associated with Al−Al bonds, but because of the additional ρ_b associated with interligand H−H and H−C noncovalent bonds, the Cp^ variant is 52.5 kJ/mol more stable. This is also why the Cp^{*Pr} variant is slightly more stable than the Cp* despite having the same amount of ρ_b associated with Al−Al bonds. The Cp^{*Pr} has roughly 20% more electron density associated with interligand H−H and H−C bonds. Clearly, interligand H−H and H−C bonds make nontrivial contributions to stability. More steric bulk does not necessarily lead to additional stability, however. Even though the Cp* variant has more steric bulk than the Cp^ variant, the Cp^ variant is slightly more stable. Despite the addition of four methyl groups to each ligand in a Cp variant, the average Al−Al distance in the resulting Cp^ variant is virtually identical (within 0.2 pm) to that of the Cp variant. The addition of a fifth methyl group, however, results in an average Al−Al distance in a Cp* variant that is 5.5 pm longer than that of a Cp variant. While the Cp* variant has more ρ_b associated with interligand bonds than the Cp^ variant, the Cp^ variant has more ρ_b associated with Al−Al bonds due to its smaller average Al−Al distance. The extra ρ_b associated with interligand bonds in the Cp* variant is not sufficient to compensate for the loss of ρ_b associated with Al−Al bonds.

Monomer/Tetramer Equilibrium. To further investigate the behavior of this series of Al(I) cyclopentadienyl compounds we examine their monomer/tetramer equilibrium in solution similar to the analysis of Huber and Schnöckel following synthesis of the Cp^ variant.[20] We used the above thermodynamic results to calculate the equilibrium constant K at room temperature for all variants using the van't Hoff equation.

$$K_{eq} = \exp(-\Delta H/RT - T\Delta S/RT) \quad (2)$$

Despite excellent agreement with tetramerization enthalpies, K values calculated via DFT differ dramatically from experiment due to the exponential dependence on ΔS. As discussed above, no computational method tested was found to predict entropy

Table 5. Experimental and Calculated Equilibrium Constants[a] at 298 K

	$Al_4Cp^{*}{}_4$	Al_4Cp_4	$Al_4Cp^{\wedge}{}_4$	$Al_4Cp^{*Et}{}_4$	$Al_4Cp^{*Pr}{}_4$	$Al_4Cp^{*iPr}{}_4$
			experimental values (T = 298K)			
ΔH_{tet}	−150				−160	−158
ΔS_{tet}	−0.300				−0.398	−0.477
K	4.1×10^{10}				1.8×10^{7}	5.8×10^{2}
ratio (mon/tet)	1:449				1:65	1:5
			calculated values (T = 298K)			
ΔH_{tet}	−148.4	−106.7	−153.1	−151.5	−158.7	−155.8
ΔS_{tet}	−0.639	−0.380	−0.437	−0.639	−0.664	−0.663
K	4.2×10^{-8}	7.0×10^{-2}	9.9×10^{3}	1.5×10^{-7}	1.3×10^{-7}	4.6×10^{-8}
			normalized K values			
K	1.0	1.7×10^{6}	2.4×10^{11}	3.5	3.2	1.1
ratio (mon/tet)	1:1	1:36	1:698	1:1.4	1:1.3	1:1

[a]ΔH_{tet} numbers are in kilojoules per mole; ΔS_{tet} numbers are in kilojoules per mole Kelvin.

DOI: 10.1021/acs.jpca.7b02075
J. Phys. Chem. A 2017, 121, 4678−4687

changes with sufficient accuracy to match experimental K values. For this reason, rather than scaling the values for ΔH_{tet} and ΔS_{tet} separately, we take the DFT results for both ΔH_{tet} and ΔS_{tet} and calculate K for each cluster before any scaling. The resulting K values are then normalized so that the result for the Cp* variant corresponds to a monomer to tetramer ratio of 1:1. Ratios for the other clusters can then be calculated from their respective normalized K values. The results, as well as experimental values, are shown in Table 5.

The experimental results for **1**, **4**, and **5** indicate there may be a trend toward preferring monomers in solution as the steric bulk of the Cp variant increases. Our computational technique, which provides a comparative estimate for the monomer/tetramer equilibrium rather than a predictive one, cannot fully distinguish these small variations between **1**, **4**, and **5**, and we can only say that Cp*, Cp^{*iPr}, Cp^{*Pr}, and Cp^{*Et} variants should have similar monomer/tetramer equilibrium. However, the calculations do show that the Cp and Cp^ systems differ from the others and are less likely to have monomers in solution. This may be of importance for alternate synthesis methods such as those reported by Roesky[14] and Fisher,[32] which can produce AlR monomers without the need for a complex co-condensation apparatus. A bias toward monomers in solution at higher temperatures may allow for greater synthetic availability of monomers in these solution-based synthesis methods. However, it appears that the complex balance between monovalent Al−Al bonding in the core and non-covalent ligand interactions in the exterior does not lead to a general trend with steric bulk but rather requires analysis of each individual system.

5. CONCLUSION

We have synthesized two new Al(I) cyclopentadienyl compounds and have used a combination of variable-temperature ^{27}Al NMR and DFT calculations to demonstrate that these are tetrameric $Al_4Cp^{*Pr}_4$ and $Al_4Cp^{*iPr}_4$. Though the thermochemistry of these systems shows a strong dependence on the DFT functional used, M06-2X/cc-pVTZ was found to predict enthalpies of tetramerization within 2% of experimental values and geometrical parameters to better than 1% of available data. Using this approach we determined the structure of the lowest-energy isomers of $Al_4Cp^{*Pr}_4$ and $Al_4Cp^{*iPr}_4$, as well as the notional $Al_4Cp^{*Et}_4$, which has yet to be synthesized. The addition of steric bulk on the Cp ligands tends to stabilize these clusters enthalpically, partly via noncovalent interactions between adjacent ligands. AIM analysis shows that there is a strong correlation between interligand bond critical points and the overall stability of the tetrameric form. However, the equilibrium in solution between monomeric and tetrameric forms does not show a simple trend with steric hindrance. Entropy changes upon tetramerization are not predicted with great accuracy by any DFT functional, and we present a simple normalization method to compare other systems to the well-studied $Al_4Cp^*_4$. Small changes in the balance between Al−Al bonding in the cluster core and noncovalent interactions between ligands can have a strong effect on the equilibrium, predominately via the entropy contribution.

■ ASSOCIATED CONTENT

Supporting Information

The Supporting Information is available free of charge on the ACS Publications website at DOI: 10.1021/acs.jpca.7b02075.

Additional details on experimental synthesis, including materials and NMR data, DFT calculations, including average bond lengths, average bond length differences, heats and entropies of tetramization, discussion of computational details, plots of calculated versus experimental chemical shifts, discussion of tetramer configurations, illustrated isomers, Atoms in Molecules details, additional plots and references. (PDF)

■ AUTHOR INFORMATION

ORCID

Joseph P. Hooper: 0000-0003-4899-1934

Notes

The authors declare no competing financial interest.

■ ACKNOWLEDGMENTS

The authors would like to thank B. Eichhorn for useful discussions. W.T. and J.H. were supported by the Office of Naval Research Multi-University Research Initiative Grant No. N0001417WX00357. D.M. and R.W. acknowledge support from the Office of Naval Research, Grant No. N0001415WX01146.

■ REFERENCES

(1) Dohmeier, C.; Robl, C.; Tacke, M.; Schnöckel, H. The Tetrameric Aluminum(I) Compound $[\{Al(\eta^5\text{-}C_5Me_5)\}_4]$. *Angew. Chem., Int. Ed. Engl.* **1991**, *30*, 564−565.

(2) Witt, M.; Roesky, H. W. Organoaluminum Chemistry at the Forefront of Research and Development. *Curr. Sci.* **2000**, *78*, 410−430.

(3) Schnöckel, H. Dalton Discussion 11: The Renaissance of Main Group Chemistry. *Dalton, Trans.* **2008**, 4344−4362.

(4) Roesky, H.; Kumar, S. Chemistry of Aluminium(I). *Chem. Commun.* **2005**, 4027−4038.

(5) Buchin, B.; Steinke, T.; Gemel, C.; Cadenbach, T.; Fischer, R. Synthesis and Characterization of the Novel Al^I Compound $Al(C_5Me_4Ph)$: Comparison of the Coordination Chemistry of $Al(C_5Me_5)$ and $Al(C_5Me_4Ph)$ at d^{10} Metal Centers. *Z. Anorg. Allg. Chem.* **2005**, *631*, 2756−2762.

(6) Ecker, A.; Weckert, E.; Schnöckel, H. Synthesis and Structural Characterization of an Al_{77}Cluster. *Nature* **1997**, *387*, 379−381.

(7) Schnepf, A.; Schnöckel, H. Metalloid Aluminum and Gallium Clusters: Element Modifications on the Molecular Scale? *Angew. Chem., Int. Ed.* **2002**, *41*, 3532−3554.

(8) Schnöckel, H.; Köhnlein, H. Synthesis and Structure of Metalloid Aluminum Clusters —Intermediates on the Way to the Elements. *Polyhedron* **2002**, *21*, 489−501.

(9) Bono, D.; Hartig, J.; Huber, M.; Schnöckel, H.; de Jongh, L. ^{27}Al NMR Study of the Metal Cluster Compound $Al_{50}C_{120}H_{180}$*. *J. Cluster Sci.* **2007**, *18*, 319−331.

(10) Schnöckel, H. Structures and Properties of Metalloid Al and Ga Clusters Open Our Eyes to the Diversity and Complexity of Fundamental Chemical and Physical Processes during Formation and Dissolution of Metals. *Chem. Rev.* **2010**, *110*, 4125−4163.

(11) Zhang, X.; Ganteför, G.; Eichhorn, B.; Mayo, D.; Sawyer, W.; Gill, A.; Kandalam, A.; Schnöckel, H.; Bowen, K. Low Oxidation State Aluminum-Containing Cluster Anions: $Cp^*Al_nH^-$, n = 1−3. *J. Chem. Phys.* **2016**, *145*, 074305.

(12) Fischer, R.; Weib, J. Coordination Chemistry of Aluminum, Gallium, and Indium at Transition Metals. *Angew. Chem., Int. Ed.* **1999**, *38*, 2830−2850.

(13) Linti, G.; Schnöckel, H. Low Valent Aluminum and Gallium Compounds — Structural Variety and Coordination Modes to Transition Metal Fragments. *Coord. Chem. Rev.* **2000**, *206−207*, 285−319.

(14) Schulz, S.; Roesky, H.; Koch, H.; Sheldrick, G.; Stalke, D.; Kuhn, A. A Simple Synthesis of $[(Cp^*Al)_4]$ and Its Conversion to the

DOI: 10.1021/acs.jpca.7b02075
J. Phys. Chem. A 2017, 121, 4678−4687

Heterocubanes $[(Cp^*AlSe)_4]$ and $[(Cp^*AlTe)_4]$ ($Cp^* = \eta^5$-$C_5(CH_3)_5$). *Angew. Chem., Int. Ed. Engl.* **1993**, *32*, 1729−1731.
(15) Purath, A.; Dohmeier, C.; Ecker, A.; Schnöckel, H.; Amelunxen, K.; Passler, T.; Wiberg, N. Synthesis and Crystal Structure of the Tetraaluminatetrahedrane $Al_4[Si(t\text{-}Bu)_3]_4$, the Second Al_4R_4 Compound. *Organometallics* **1998**, *17*, 1894−1896.
(16) Schnitter, C.; Roesky, H.; Röpken, C.; Herbst-Irmer, R.; Schmidt, H.; Noltemeyer, M. The Behavior of $[RAlX_2\cdot THF]$ Compounds under Reductive Conditions: Tetrakis[tris(trimethylsilyl)methylaluminum(I)] − A Neutral Aluminum(I) Compound with σ-Bound Alkyl Groups and a Tetrahedral Structure. *Angew. Chem., Int. Ed.* **1998**, *37*, 1952−1955.
(17) Sitzmann, H.; Lappert, M.; Dohmeier, C.; Üffing, C.; Schnöckel, H. Cyclopentadienylderivate von Aluminium(I). *J. Organomet. Chem.* **1998**, *561*, 203−208.
(18) Schiefer, M.; Reddy, N.; Roesky, H.; Vidovic, D. Synthesis and Structural Characterization of an Exclusively N-Based Tetrameric Aluminum(I) Compound. *Organometallics* **2003**, *22*, 3637−3638.
(19) Purath, A.; Schnöckel, H. Tetrakis[tris(trimethylsilyl)-silylaluminium(I)] $Al_4[Si(SiMe_3)3]_4$—eine siliziumreicheVerbindung mit zentralem tetraedrischem Al_4-Kern. *J. Organomet. Chem.* **1999**, *579*, 373−375.
(20) Huber, M.; Schnöckel, H. $Al_4(C_5Me_4H)_4$: Structure, Reactivity and Bonding. *Inorg. Chim. Acta* **2008**, *361*, 457−461.
(21) Ahlrichs, R.; Ehrig, M.; Horn, H. Bonding in the Aluminum Cage Compounds $[Al(\eta^5\text{-}C_5R_5)]_4$ and Al_4X_4, X = H, F, Cl. *Chem. Phys. Lett.* **1991**, *183*, 227−233.
(22) Schneider, U.; Ahlrichs, R.; Horn, H.; Schäfer, A. Ab lnitio Investigations of Structure and Stability of $[R_3SiAl]_4$ R = H, Me, *t*Bu. *J. Angew. Chem., Int. Ed. Engl.* **1992**, *31*, 353−355.
(23) Dohmeier, C.; Loos, D.; Schnöckel, H. Aluminum(I) and Galium(I) Compounds: Syntheses, Structure and Reactions. *Angew. Chem., Int. Ed. Engl.* **1996**, *35*, 129−149.
(24) Alary, F.; Heully, J.-L.; Poteau, R.; Maron, L.; Trinquier, G.; Daudey, J.-P. Using Effective Group Potential Methodology for Predicting Organometallic Complex Properties. *J. Am. Chem. Soc.* **2003**, *125*, 11051−11061.
(25) Vollet, J.; Hartig, J. R.; Schnöckel, H. $Al_{50}C_{120}H_{180}$: A Pseudofullerene Shell of 60 Carbon Atoms and 60 Methyl Groups Protecting a Cluster Core of 50 Aluminum Atoms. *Angew. Chem., Int. Ed.* **2004**, *43*, 3186−3189.
(26) Huber, M.; Henke, P.; Schnöckel, H. Experimentally Based DFT Calculations on the Hindered Disproportionation of $[Al_4Cp^*_4]$: Formation of Metalloid Clusters as Intermediates on the Way to Solid Al Prevents the Decomposition of a Textbook Molecule. *Chem. - Eur. J.* **2009**, *15*, 12180−12183.
(27) Stelzer, A. C.; Hrobárik, P.; Braun, T.; Kaupp, M.; Braun-Cula, B. Completing the Heterocubane Family $[Cp^*AlE]_4$ (E = O, S, Se, and Te) by Selective Oxygenation and Sulfuration of $[Cp^*Al]_4$: Density Functional Theory Calculations of $[Cp^*AlE]_4$ and Reactivity of $[Cp^*AlO]_4$ toward Hydrolysis. *Inorg. Chem.* **2016**, *55*, 4915−4923.
(28) Williams, K.; Hooper, J. P. Structure, Thermodynamics, and Energy Content of Aluminum Cyclopentadienyl Clusters. *J. Phys. Chem. A* **2011**, *115*, 14100−14109.
(29) Lu, F.; Li, X.; Sun, Z.; Zeng, Y.; Meng, L. Influences of the Substituents on the M−M Bonding in Cp_4Al_4 and $Cp_2M_2X_2$ (M = B, Al, Ga; Cp = C_5H_5, X = halogen). *Dalton, Trans.* **2015**, *44*, 14092−14100.
(30) Wagner, J.; Schreiner, P. London Dispersion in Molecular Chemistry- Reconsidering Steric Effects. *Angew. Chem., Int. Ed.* **2015**, *54*, 12274−12296.
(31) Guo, J.; Liptrot, D.; Nagase, S.; Power, P. The Multiple Bonding in Heavier Group 14 Element Alkene analogues is Stabilized Mainly by Dispersion Force Effects. *Chem. Sci.* **2015**, *6*, 6235−6244.
(32) Ganesamoorthy, C.; Loerke, S.; Gemel, C.; Jerabek, P.; Winter, M.; Frenking, G.; Fischer, R. Reductive Elimination: A Pathway to Low-Valent Aluminium Species. *Chem. Commun.* **2013**, *49* (28), 2858.
(33) Frisch, M. J.; et al. *Gaussian 09,* Revision E01; Gaussian Inc.: Wallingford, CT, 2009.
(34) Grimme, S.; Antony, J.; Ehrlich, S.; Krieg, H. A Consistent and Accurate *ab initio* Parametrization of Density Functional Dispersion Correction (DFT-D) for the 94 Elements H-Pu. *J. Chem. Phys.* **2010**, *132*, 154104.
(35) Kohout, M. *DGrid, Version 4.6;* Springer, 2014.
(36) Wolinski, K.; Hinton, J.; Pulay, P. Efficient Implementation of the Gauge-Independent Atomic Orbital Method for NMR Chemical Shift Calculations. *J. Am. Chem. Soc.* **1990**, *112*, 8251−8260.
(37) Goerigk, L.; Grimme, S. Efficient and Accurate Double-Hybrid-Meta-GGA Density Functionals—Evaluation with the Extended GMTKN30 Database for General Main Group Thermochemistry, Kinetics, and Noncovalent Interactions. *J. Chem. Theory Comput.* **2010**, *6*, 107−126.
(38) Kruse, H.; Goerigk, L.; Grimme, S. Why the Standard B3LYP/6-31G* Model Chemistry Should Not Be Used in DFT Calculations of Molecular Thermochemistry: Understanding and Correcting the Problem. *J. Org. Chem.* **2012**, *77*, 10824−10834.
(39) Zhao, Y.; Truhlar, D. The M06 Suite of Density Functionals for Main Group Thermochemistry, Thermochemical Kinetics, Noncovalent Interactions, Excited States, and Transition Elements: Two New Functionals and Systematic Testing of Four M06-Class Functionals and 12 Other Functionals. *Theor. Chem. Acc.* **2008**, *120*, 215−241.
(40) Becke, A. Density-Functional Exchange-Energy Approximation with Correct Asymptotic-Behavior. *Phys. Rev. A: At., Mol., Opt. Phys.* **1988**, *38*, 3098−3100.
(41) Perdew, J. Density-Functional Approximation for the Correlation Energy of the Inhomogeneous Electron Gas. *Phys. Rev. B: Condens. Matter Mater. Phys.* **1986**, *33*, 8822−8824.
(42) Becke, A. Density-Functional Thermochemistry. III. The Role of Exact Exchange. *J. Chem. Phys.* **1993**, *98*, 5648−5652.
(43) Tao, J.; Perdew, J.; Staroverov, V.; Scuseria, G. Climbing the Density Functional Ladder: Nonempirical Meta−Generalized Gradient Approximation Designed for Molecules and Solids. *Phys. Rev. Lett.* **2003**, *91*, 146401.
(44) Perdew, J.; Burke, K.; Ernzerhof, M. Generalized Gradient Approximation Made Simple. *Phys. Rev. Lett.* **1996**, *77*, 3865−3868.
(45) Adamo, C.; Barone, V. Toward Reliable Density Functional Methods without Adjustable Parameters: The PBE0Model. *J. Chem. Phys.* **1999**, *110*, 6158−6169.
(46) Zhao, Y.; Truhlar, D. A New Local Density Functional for Main-Group Thermochemistry, Transition Metal Bonding, Thermochemical Kinetics, and Noncovalent Interactions. *J. Chem. Phys.* **2006**, *125*, 1−18.
(47) Adamo, C.; Barone, V. Exchange Functionals with Improved Long-Range Behavior and Adiabatic Connection Methods without Adjustable Parameters: The *m*PW and *m*PW1PW Models. *J. Chem. Phys.* **1998**, *108*, 664−675.
(48) Austin, A.; Petersson, G.; Frisch, M.; Dobek, F.; Scalmani, G.; Throssell, K. A Density Functional with Spherical Atom Dispersion Terms. *J. Chem. Theory Comput.* **2012**, *8*, 4989.
(49) McLean, A.; Chandler, G. Contracted Gaussian Basis Sets for Molecular Calculations. I. Second Row Atoms, *Z* = 11−18. *J. Chem. Phys.* **1980**, *72*, 5639−5648.
(50) Clark, T.; Chandrasekhar, J.; Spitznagel, G.; Schleyer, P. Efficient Diffuse Function-Augmented Basis Sets for Anion Calculations. III. The 3-21+G Basis Set for First-Row Elements, Li−F. *J. Comput. Chem.* **1983**, *4*, 294−301.
(51) Weigend, F.; Ahlrichs, R. Balanced Basis Sets of Split Valence, Triple Zeta Valence and Quadruple Zeta Valence Quality for H to Rn: Design and Assessment of Accuracy. *Phys. Chem. Chem. Phys.* **2005**, *7*, 3297−3305.
(52) Schaefer, A.; Horn, H.; Ahlrichs, R. Fully Optimized Contracted Gaussian Basis Sets for Atoms Li to Kr. *J. Chem. Phys.* **1992**, *97*, 2571−2577.
(53) Francl, M. M.; Pietro, W. J.; Hehre, W. J.; Binkley, J. S.; DeFrees, D. J.; Pople, J. A.; Gordon, M. S. Self-Consistent Molecular Orbital Methods. XXIII. A Polarization-Type Basis Set for Second-Row Elements. *J. Chem. Phys.* **1982**, *77*, 3654−3665.

DOI: 10.1021/acs.jpca.7b02075
J. Phys. Chem. A 2017, 121, 4678−4687

(54) Dunning, T. H. Gaussian Basis Sets for use in Correlated Molecular Calculations. I. The Atoms Boron Through Neon and Hydrogen. *J. Chem. Phys.* **1989**, *90*, 1007−1023.
(55) Boys, S.; Bernardi, F. The Calculation of Small Molecular Interactions by the Differences of Separate Total Energies. Some Procedures with Reduced Errors. *Mol. Phys.* **1970**, *19*, 553−566.
(56) Klamt, A.; Schüürmann, G. COSMO: A New Approach to Dielectric Screening in Solvents with Explicit Expressions for the Screening Energy and its Gradient. *J. Chem. Soc., Perkin Trans. 2* **1993**, 799−805.
(57) Barone, V.; Cossi, M. Quantum Calculation of Molecular Energies and Energy Gradients in Solution by a Conductor Solvent Model. *J. Phys. Chem. A* **1998**, *102*, 1995−2001.
(58) Thanthiriwatte, K.; Hohenstein, E.; Burns, L.; Sherrill, C. Assessment of the Performance of DFT and DFT-D Methods for Describing Distance Dependance of Hydrogen-Bonded Interactions. *J. Chem. Theory Comput.* **2011**, *7*, 88−96.
(59) Burns, L.; Vázquez-Mayagoitia, Á.; Sumpter, B.; Sherrill, C. Density-functional Approaches to Noncovalent Interactions: A Comparison of Dispersion Corrections (DFT-D), Exchange-hole Dipole Moment (XDM) Theory, and Specialized Functionals. *J. Chem. Phys.* **2011**, *134*, 084107.
(60) Goerigk, L.; Kruse, H.; Grimme, S. Benchmarking Density Functional Methods against the S66 and S66 × 8 Datasets for Non-Covalent Interactions. *ChemPhysChem* **2011**, *12*, 3421−3433.
(61) Grabowski, S. An Estimation of Strength of Intramolecular Hydrogen Bonds − ab initio and AIM Studies. *J. Mol. Struct.* **2001**, *562*, 137−143.
(62) Grabowski, S. High-Level Ab Initio Calculations of Dihydrogen-Bonded Complexes. *J. Phys. Chem. A* **2000**, *104*, 5551−5557.
(63) Cortés-Guzmán, F.; Bader, R. Complementarity of QTAIM and MO Theory in the Study of Bonding in Donor−Acceptor Complexes. *Coord. Chem. Rev.* **2005**, *249*, 633−662.
(64) Boyd, R.; Choi, S. Hydrogen Bonding Between Nitriles and Hydrogen Halides and the Topological Properties of Molecular Charge Distributions. *Chem. Phys. Lett.* **1986**, *129*, 62−65.

DOI: 10.1021/acs.jpca.7b02075
J. Phys. Chem. A 2017, 121, 4678−4687